
SPARSE AND TRANSFERABLE UNIVERSAL SINGULAR VECTORS ATTACK

A PREPRINT

Kseniia Kuvshinova^{1,4*†} Olga Tsimboi^{1,2*} Ivan Oseledets^{3,4}

¹Sber AI Lab, Moscow, Russia

²Moscow Institute of Physics and Technology, Moscow, Russia

³Artificial Intelligence Research Institute (AIRI), Moscow, Russia

⁴Skolkovo Institute of Science and Technology, Moscow, Russia

kse.kuvshinova@gmail.com, tsimboi. oa@phystech.edu, oseledets@airi.net

ABSTRACT

The research in the field of adversarial attacks and models' vulnerability is one of the fundamental directions in modern machine learning. Recent studies reveal the vulnerability phenomenon, and understanding the mechanisms behind this is essential for improving neural network characteristics and interpretability. In this paper, we propose a novel sparse universal white-box adversarial attack. Our approach is based on truncated power iteration providing sparsity to (p, q) -singular vectors of the hidden layers of Jacobian matrices. Using the ImageNet benchmark validation subset, we analyze the proposed method in various settings, achieving results comparable to dense baselines with more than a 50% fooling rate while damaging only 5% of pixels and utilizing 256 samples for perturbation fitting. We also show that our algorithm admits higher attack magnitude without affecting the human ability to solve the task. Furthermore, we investigate that the constructed perturbations are highly transferable among different models without significantly decreasing the fooling rate. Our findings demonstrate the vulnerability of state-of-the-art models to sparse attacks and highlight the importance of developing robust machine learning systems.

1 Introduction

In recent years, deep learning approaches have become increasingly popular in many areas and applications, starting from computer vision Dosovitskiy et al. [2021a] and natural language processing Touvron et al. [2023], Chung et al. [2022] to robotics Roy et al. [2021] and speech recognition Baevski et al. [2020]. The success and availability of pre-trained neural networks have also made it easier for researchers and developers to use these models for their applications. Despite tremendous advances, it was discovered that deep learning models are vulnerable to small perturbations of input data called adversarial attacks that mislead models and cause incorrect predictions Szegedy et al. [2014], Goodfellow et al. [2014], Moosavi-Dezfooli et al. [2017]. Adversarial attacks as a phenomenon first appeared in the field of computer vision and have raised concerns about the reliability in safety-critical machine learning applications.

Initially, adversarial examples were constructed for each individual input Szegedy et al. [2014], making it challenging to scale attacking methods to large datasets. In Moosavi-Dezfooli et al. [2017], the authors show the existence of universal adversarial perturbations (UAPs) that result in the model's misclassification for most of the inputs. Such attacks are crucial for adversarial machine learning research, as they are easier to deploy in real-world applications and raise questions about the safety and robustness of state-of-the-art architectures. However, the proposed optimization algorithm requires vast data, making it complicated to fool real-world systems. In contrast, Khrulkov and Oseledets [2018] proposes a sample-efficient method to construct perturbation using leading (p, q) -singular vectors Boyd [1974]

*These authors contributed equally to this work.

†Corresponding author.

of the Jacobian of the hidden layer. However, Jacobian is infeasible directly due to the memory limitation, the authors overcome this issue using the generalized power method for the attack computation.

Above approaches formalize imperceptibility using straightforward vector norm constraints in the underlying optimization problem. However, in general, an attack can alter the image significantly, leaving its semantics unchanged Song et al. [2018], Brown et al. [2018]. One can step beyond the small-norm imperceptibility definition and perform a patch attack as a physical sticker on an object in real-time conditions Hu and Shi [2022], Li et al. [2019], Pautov et al. [2019], Kaziakhmedov et al. [2019]. In this work, we focus on attacks under sparsity constraints. Indeed, damaging a small number of pixels does not significantly influence image semantics and hence human perception, resulting in unchanged prediction.

There are quite a lot methods to compute sparse adversaries Croce and Hein [2019], Modas et al. [2019], Yuan et al. [2021], Dong et al. [2020], however, the transferability of l_0 - bounded attacks is still low Papernot et al. [2016], He et al. [2022], Zhang et al. [2023]. In other words, these methods may perform poorly in grey-box settings (when, instead of the initial model, a surrogate model is attacked). However, we should highlight that only a few works aim to incorporate sparsity constraints into universal attack setup Shafahi et al. [2020], Croce et al. [2022]. More than that, an auxiliary generative model is usually used to construct such transferable sparse attacks He et al. [2022], Hayes and Danezis [2018], Mopuri et al. [2018].

The main focus of this paper is to investigate computer vision models’ robustness to sparse universal adversarial examples. Summing up, our main contribution is as follows:

- We propose a new approach to construct sparse UAPs on hidden layers subject to predefined cardinality or sparsity patterns.
- We assess our method on the ImageNet benchmark dataset Deng et al. [2009a] and evaluate it on various deep learning models. We compare it against existing universal approaches regarding the fooling rate and the transferability between models.
- In our experimental study, we show that the proposed method produces highly transferable perturbations. It is important that our approach is efficient with respect to sample size – a moderate sample size of 256 images to construct an attack on is enough for a reasonable attack fooling rate.

2 Framework

In this paper, we focus on the problem of untargeted universal perturbations for image classification. The problem of universal adversarial attacks can be framed as finding a perturbation ε that, when added to most input images x , causes the classifier to predict a different class than it would for the original images. Let $f : \mathcal{X} \rightarrow \mathcal{Y}$ be a classification model defined for the dataset $\mathcal{D} = \{x_i, y_i\}_{i=1}^N$, where x_i is an input and y_i is a corresponding label, then, according to Moosavi-Dezfooli et al. [2016a], UAP is a perturbation ε such that

$$\mathbb{P}_{x \sim \mu}[f(x + \varepsilon) \neq f(x)] \geq 1 - \delta, \quad \|\varepsilon\| \leq \xi,$$

where μ denotes a distribution of input data, $1 - \delta$ is the minimal Fooling Rate (FR) and ξ is the attack magnitude. It should be highlighted that this perturbation must not change human prediction, meaning that the true class of the attacked image remains unchanged, but a small norm constraint could be omitted Song et al. [2018], Brown et al. [2018].

Adversarial perturbations are often obtained via optimization problem solution. The most straightforward approach is to maximize expected cross-entropy loss $\mathcal{L}(x + \varepsilon, y)$. It was shown Khrukov and Oseledets [2018] that instead of attacking the model output, one can attack hidden layers of a model. Then the error produced in this way propagates to the last network layer, resulting in a model prediction change. Given the i -th layer l , the optimization problem, in this case, can be obtained via Taylor expansion:

$$\begin{aligned} l(x + \varepsilon) - l(x) &\approx J_i(x)\varepsilon \\ \|l(x + \varepsilon) - l(x)\|_q^q &\rightarrow \max_{\|\varepsilon\|_p \leq \xi}, \end{aligned} \quad (1)$$

where $J_i(x)$ is the i -th layer Jacobian operator and $J_i(x)\varepsilon$ is Jacobian action on ε . Finally, (1) is equivalent to the following problem.

$$\max_{\varepsilon} \mathbb{E}_{x \sim \mu} \|J_i(x)\varepsilon\|_q^q, \quad s.t. \|\varepsilon\|_p = 1. \quad (2)$$

The solution to (2) can be referred to as Jacobian (p, q) -singular vector and defined up to the signed scale factor, here p, q are the hyperparameters to be tuned, and expectation is relaxed via averaging over a batch.

Our approach. In this paper, we incorporate the universal layerwise approach from above with sparsity or, formally speaking, additional non-convex l_0 constraint:

$$\begin{aligned} & \sum_{x \in \text{batch}} \|J_i(x)\varepsilon\|_q^q \rightarrow \max, \\ & \text{s.t. } \|\varepsilon\|_p = 1, \quad \|\varepsilon\|_0 \leq k. \end{aligned} \quad (3)$$

In the case when $p = q = 2$, the problem above leads to the famous problem of finding sparse eigenvalues. However, for an arbitrary pair (p, q) , it is a non-convex and NP-hard problem. One way to obtain an approximate solution is to use the truncated power iteration method (TPower, Yuan and Zhang [2013]). This method can effectively recover the sparse eigenvector for symmetric positive semidefinite matrices and when the underlying matrix admits sparse eigenvectors. Despite efficiency and simplicity, the major TPower drawback is the theoretical guarantee with a narrow convergence region. One way to reduce the effect of this issue is to reduce the number of nonzero entries iteratively.

In this paper, we introduce an algorithm that adopts TPower for the case of arbitrary p, q and effectively solves the problem of universal perturbation finding.

Let us rewrite (3) using the dual norm definition, then we obtain

$$\max_{\varepsilon \in \mathcal{B}_p(1)} \max_{y \in \mathcal{B}_{q^*}(1)} y^\top J_i \varepsilon, \quad \text{s.t. } \|\varepsilon\|_0 \leq k, \quad (4)$$

where $(q^*)^{-1} + q^{-1} = 1$, $\mathcal{B}_p(1) = \{x \in \mathbb{R}^n \mid \|x\|_p = 1\}$ and $J_i = [J_i(x_1)^\top, \dots, J_i(x_N)^\top]^\top$, $x_j \in \text{batch}$. The solution could be found via Alternating Maximization (AM) Method.

For any fixed perturbation vector ε , the inner problem is linear and admits a closed-form solution, using $b = J_i \varepsilon$ for notation, we have:

$$y = \frac{\psi_q(b)}{\|\psi_q(b)\|_{q^*}}, \quad \psi_q(y) = \text{sign}(y)|y|^{q-1}. \quad (5)$$

Changing the order of maximizations in (4), the subproblem for ε remains the same except l_0 constraint, which could be replaced by additional binary variable t maximization. Thus, denoting $d = J_i^\top y$, we have:

$$\max_{\varepsilon \in \mathcal{B}_p(1)} d^\top \varepsilon, \quad \text{s.t. } \|\varepsilon\|_0 \leq k. \quad (6)$$

$$\max_t \max_{\varepsilon \in \mathcal{B}_p(1)} (t \cdot d)^\top \varepsilon, \quad \text{s.t. } t_j \in \{0, 1\}, \forall j. \quad (7)$$

here (\cdot) is a Hadamar product.

For a fixed t , the problem is reduced to the previous case, and hence

$$\varepsilon \sim \psi_{p^*}(t \cdot d), \quad (8)$$

Now, substituting this equation to the objective (7), we derive:

$$(t \cdot d)^\top \varepsilon = d^\top \text{diag}(t) |d|^{p^*-1} \text{sign}(d) = \sum_j |d_j| |d_j|^{p^*-1} t_j = \sum_j |d_j|^{p^*} t_j \rightarrow \max_t$$

and thus maximization by t is simply a selection of the greatest components of vector d in absolute value, which could be done by truncation operator:

$$T_{p^*,k}(d) = \begin{cases} d_i, & i \in \text{ArgTop}_k\{\|d_i\|_{p^*}\}, \\ 0, & \text{otherwise,} \end{cases} \quad (9)$$

here $\|\cdot\|_{p^*}$ is used to emphasize the possibility of a block-sparse solution under the predefined sparsity pattern for patch attack.

Finally, putting it together, we derive the following alternating maximization update at the step s for attack training.:

$$\varepsilon^{s+1} = T_{p^*,k} \left[\sum_{x \in \text{batch}} J_i^\top(x) \psi_q(J_i(x)\varepsilon^s) \right], \quad (10)$$

$$\varepsilon^{s+1} = \frac{\psi_{p^*}(\varepsilon^{s+1})}{\|\psi_{p^*}(\varepsilon^{s+1})\|_p}. \quad (11)$$

The overall algorithm is presented in Algorithm 1, where we gradually decrease the cardinality through the iterations to enhance convergency.

Algorithm 1: TPower Attack

Require: $n_steps, init_truncation \in (0, 1)$, batch of images $x_j \in \mathbb{R}^{n \times n \times \text{channels}}$, $j \in \overline{1, N}$, q, p , target cardinality $top_k, patch_size, reduction_steps$.

- 1: $k = init_truncation \cdot (n/patch_size)^2 \cdot \text{channels}$.
- 2: $k = \max(k, top_k)$.
- 3: $\varepsilon =$ random tensor of batch size.
- 4: **for** s from 1 to n_steps **do**
- 5: $\varepsilon^{s+1} = T_{p^*, k} \left[\sum_{x \in \text{batch}} J_i^\top(x) \psi_q(J_i(x) \varepsilon^s) \right]$, (10)
- 6: $\varepsilon^{s+1} = \frac{\psi_{p^*}(\varepsilon^{s+1})}{\|\psi_{p^*}(\varepsilon^{s+1})\|_p}$, (11)
- 7: **if** $s \bmod reduction_steps = 0$ **then**
- 8: $k_{\text{reduction}} = \text{pow}(\frac{k}{top_k}, \frac{reduction_steps}{n_steps})$
- 9: $k = \max(k/k_{\text{reduction}}, top_k)$
- 10: **end if**
- 11: **end for**

Ensure: ε

3 Experiments

This section presents the experiments conducted to analyze the effectiveness of sparse UAPs described above. The experiments were implemented using PyTorch, and the code will be made publicly available on Github upon publication.

3.1 Experiments setup

Datasets. In this work, following Khruikov and Oseledets [2018], to evaluate the performance of the proposed sparse attack, we used the validation subset of the ImageNet benchmark dataset (ILSVRC2012, Deng et al. [2009b]), which contains 50,000 images belonging to 1,000 object categories. We randomly sample 256 images from the ImageNet validation subset for attack training. Additionally, to perform grid search, there were stratified sampled 5000 images as a validation set, while the rest of the samples were used as the test set.

Models. During the empirical analyses, we restrict ourselves to the following models to be examined: DenseNet161 Huang et al. [2017], EfficientNetB0, EfficientNetB3 Tan and Le [2019], InceptionV3 Szegedy et al. [2015], ResNet101, ResNet152 He et al. [2016], VGG19 Simonyan and Zisserman [2015], Wide ResNet101 Zagoruyko and Komodakis [2016], DEiT base Touvron et al. [2021], ViT base Dosovitskiy et al. [2021b]. For each model, there were used ImageNet pre-trained checkpoints.

Hyperparameters. In our experiments, to estimate attack performance, we vary the following hyperparameters: model, layer to be attacked, patch size $\in \{1, 4, 8\}$ and objective norm parameter $q \in \{1, 2, 3, 5, 7, 10\}$ while keeping p fixed, in particular, $p = \infty$ which is motivated by the previous study Khruikov and Oseledets [2018]. The number of non-zero patches k is also fixed in accordance with the image and patch sizes and selected so that the fraction of damaged pixels is equal to 5%, which further allows us to increase the attack magnitude up to 1 (Table 1). We gradually went through all semantic blocks to study the performance dependence on the layer to be attacked (see Appendix for more details).

We performed the computation on four GPU’s NVIDIA A100 of 80GB. The full grid search for TPower Attack took 765 GPU hours for nine models in total (6 values for q , ten values for α and three patch sizes).

Evaluation metrics. For evaluation, we report Fooling Rate (FR) (12) on the validation and test subsets for the best perturbation obtained on the 256 training samples. It also means that we find ourselves in an unsupervised setting and do not need access to the ground truth labels.

$$FR = \frac{1}{N} \sum_{x \in \mathcal{D}} [f(x) \neq f(x + \varepsilon)] \quad (12)$$

Along with fooling rate, we focus our consideration on Attack Success Rate (ASR), namely the portion of misclassified samples after the attack performance filtered subject to the initial model’s correct predictions:

$$ASR = \frac{\sum_{x \in \mathcal{D}} [f(x) \neq f(x + \varepsilon)][f(x) = y]}{\sum_{x, y \in \mathcal{D}} [f(x) = y]} \quad (13)$$

3.2 Main results

We train our attack on nine different models and compare it to the stochastic gradient descent (SGD) attack Shafahi et al. [2020] and the dense analogue of our approach proposed by Khruikov and Oseledets [2018], here and below, we refer the last approach as singular vectors (SV) attack. We also consider transferability setup and discover the FR dependence on q . Following previous research, which relies on the small norm assumption, the magnitude was decreased to $10/255$ for dense baselines. Our approach is significantly superior to dense attacks. Poor results in the SGD can be explained by the fact that a relatively large train set size is required to obtain an efficient attack (e.i. greater than the number of classes), while for our proposed approach, 256 images are enough.

The results of the grid search are presented in Table 1, where we report optimal hyperparameters for each model with respect to validation FR. For this setting, the comparison with the baselines is provided in Table 2, where for SV attack, we additionally perform a similar grid search on the layer and q .

Model	Top k	Patch Size	q	Attacked Layer	Test ASR	Test FR
DenseNet161	2509	1	1	features.denseblock2.denselayer6	87.61	89.11
EfficientNetB0	2509	1	1	features.2.1.block	29.66	37.09
EfficientNetB3	4500	1	1	features.1.0.block	9.66	15.22
InceptionV3	4471	1	1	maxpool2	82.83	85.04
ResNet101	157	4	1	layer2.3	93.8	94.57
ResNet152	157	4	1	layer2.3	94.24	94.84
WideResNet101	157	4	1	layer3.1	93.71	94.36
DEIT base	2509	1	1	vit.encoder.layer.0	36.12	43.37
ViT base	2509	1	1	vit.encoder.layer.0	46.76	52.5

Table 1: Metrics and hyperparameters for the best-performed sparse UAPs for each model.

Our TPower attack approach outperforms baselines for almost all models except EfficientNets and demonstrates diverse attack patterns.

From Table 2, one can conclude that EfficientNet is the most robust architecture. Some architectural choices, like compound scaling, limit the gradient flow during backpropagation. This fact makes it more challenging for attackers to generate efficient adversarial perturbations. It is worth mentioning that the attack training on EfficientNets results in noticeably different perturbation patterns than other models. It is more similar to white noise (see Figure 1), whereas the distribution of the patches trained on other models resembles higher order Sobol points Sobol’ [1967]. Additionally, for the ViT model, Figure 1 demonstrates a highly interpretable pattern. Formally speaking, during ViT preprocessing, the image is cut into fixed-size patches, which are further flattened and combined with positional encoding Wu et al. [2020]. Indeed, perturbation forms a quasi-regular grid repeating the locations of the patch junctions. Moreover, attacking lower, more sensitive to preprocessing by construction layers causes the highest model vulnerability (Figure 4).

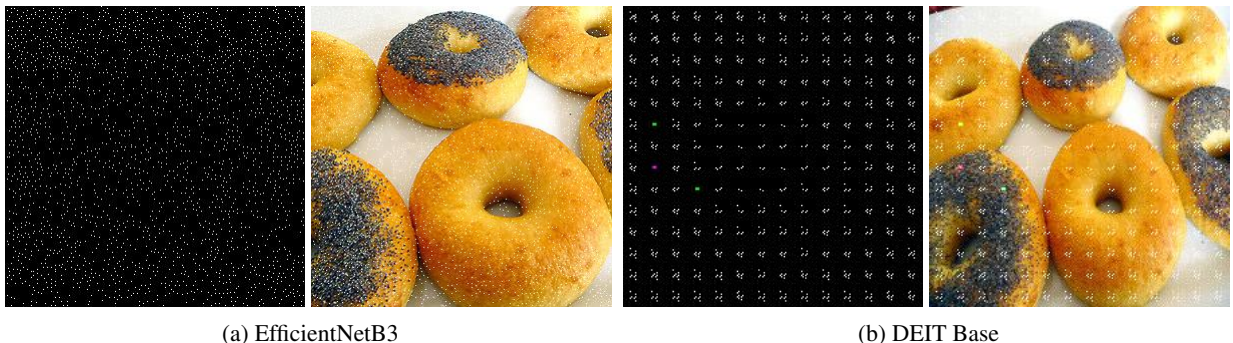


Figure 1: Sparse UAPs obtained using the TPower algorithm and corresponding examples of attacked images. Perturbations were computed using the best-performed layers on gridsearch.

Dependence on patch size. Our empirical study shows that, in general, lower patch size values are more beneficial in terms of FR (see Table 1). One can see that pixel-wise attack mode is more efficient regarding the fooling rate. This might be related to the fact that uniform square greed is not an optimal sparsity pattern. However, for most models, the decrease in performance is not dramatic, except for the transformers one. For those models where the optimal patch size

Model	Ours	SV	SGD	LMax
DenseNet161	89.11	34.25	15.53	22.70
EfficientNetB0	37.09	34.44	16.35	-
EfficientNetB3	15.22	13.49	8.22	11.10
InceptionV3	85.04	27.88	13.11	23.63
ResNet101	94.57	50.05	17.17	44.51
ResNet152	94.84	35.93	15.05	20.12
WideResNet101	94.36	36.35	15.02	26.56
DEIT base	43.37	31.1	19.16	23.61
ViT base	52.5	26.01	17.09	29.54

Table 2: Comparison between TPower (Ours), SV and SGD adversarial perturbations. For the TPower and SV attack, there reported the test Fooling Rate (FR) for optimal hyperparameters after the gridsearch.

Model / Patch size	1	4	8
DenseNet161	89.11	78.52	64.82
EfficientNetB0	37.09	29.95	22.87
EfficientNetB3	15.22	13.11	13.28
InceptionV3	85.04	22.36	77.66
ResNet101	89.85	94.57	83.48
ResNet152	89.53	94.84	76.78
WideResNet101	93.97	94.36	84.1
DEIT base	43.37	22.37	15.59
ViT base	52.5	15.44	14.54

Table 3: Tpower attack Fooling Rate (FR) dependence on patch size on test for frozen other optimal hyperparameters.

option is 4, FR does not decrease significantly compared to the single pixel patch attack, namely, only approximately 5% for ResNet101 (from 94.57% to 89.85%, 3). Finally, the small size of patches with a fixed proportion of damaged pixels allows patches to scatter more across the whole picture, resulting in more uniform perturbation of model filters' receptive fields.

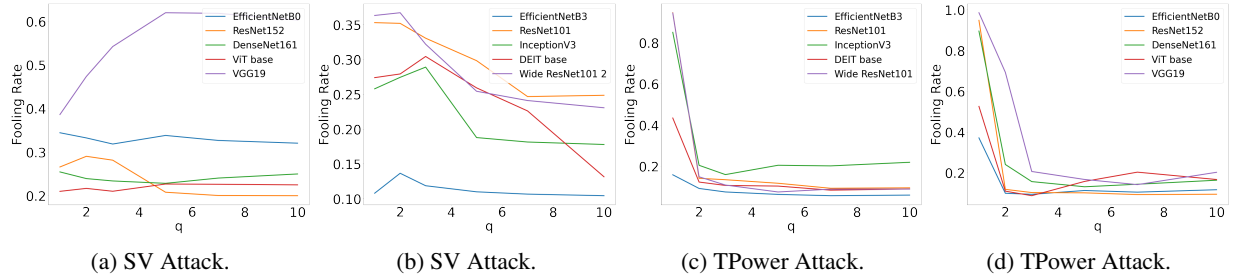


Figure 2: Dependence of Fooling Rate (FR) on q for TPower Attack. For sparse attacks, optimal parameters from gridsearch were frozen except for q (see Table 1) and reused for the dense one.

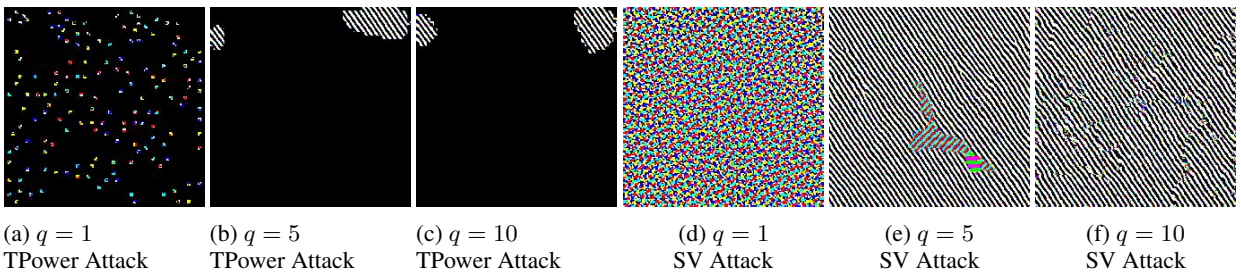


Figure 3: Universal adversarial perturbations constructed for the VGG19 model.

Dependence on q . In Khrulkov and Oseledets [2018], on the example of VGG19, authors demonstrate that model vulnerability increases with q and saturates when $q = 5$. The last is explained by the fact that $q = 5$ is enough to smooth the approximation of $q = \infty$. On the contrary, for the majority of models, we obtained almost opposite results: higher q values are less efficient in terms of FR for both methods, ours and the SV attack (see Figure 2). However, for the sparse attack setting, all models' dependence becomes unambiguous even for the VGG19 model. In addition, with $q = 1$, patches are arranged more evenly across the perturbation image than for larger values of q , which is depicted in Figure 3.

Dependence on layer number. In our experiments, to investigate attack performance depending on a layer, we introduce layer ratio: the layer number normalized to the model depth. From Figure 4, one can observe that lower

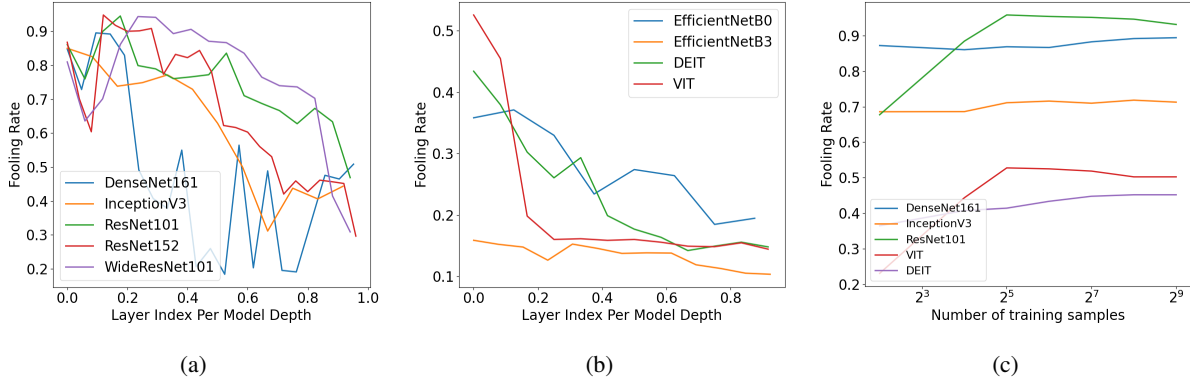


Figure 4: 4a and 4b: Fooling Rate (FR) dependence on layer ratio for examined models. 4c: The example of fooling rate saturation depending on training set size for optimal hyperparameters; here, one can observe that 256 is the worst case amount among most vulnerable models.

layers are more effective, empirically confirming the hypothesis of perturbation propagation through the network and repeating the SV attack property.

Cardinality experiments. We analyzed one of the critical hyperparameters - the number of adversarial patches denoted k . This hyperparameter plays a pivotal role in determining the ratio of damaged pixels of the attack, as well as the overall performance of the attack. In the initial experiments, we selected the k parameter following the 5% rate of affected pixels, producing promising results on our dataset. We conducted an additional experiment to determine how many sparse adversarial patches are enough to obtain the same fooling rate as for the dense attack. Figure 5 illustrates the resulting images for four models. As anticipated, the choice of k significantly affects the attack performance. However, from Table 4, one can conclude that less than 1% of pixels is enough to obtain an equally efficient attack with SV one.

Model	%	Model	%
InceptionV3	0.56	ResNet152	0.27
DenseNet161	0.5	ResNet101	0.37

Table 4: The percentage of pixels required for TPower attack to achieve approximately the same FR as SV attack (see Table 2).

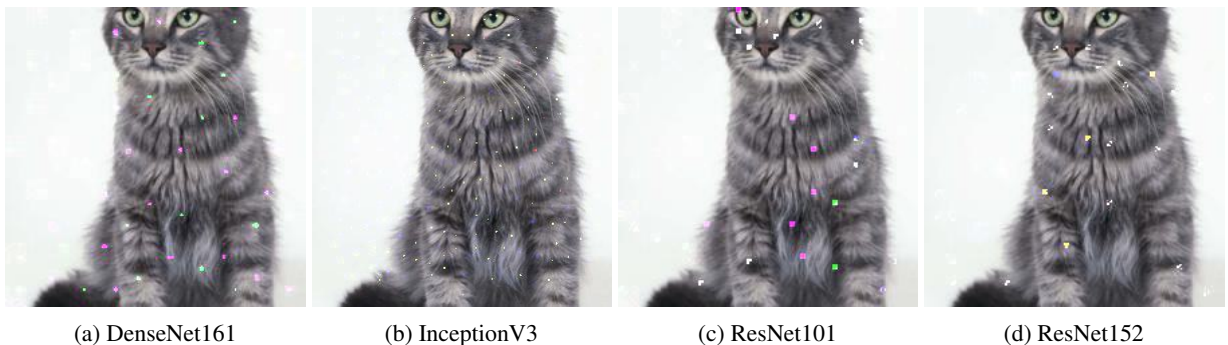


Figure 5: UAPs and corresponding attacked images obtained using our TPower approach. The k parameter was manually selected such that sparse UAPs reach approximately the same validation Fooling Rate (FR) as SV attacks.

Median filtration. As mentioned above, the constructed perturbations consist of full-magnitude damaged patches scattered uniformly on the image. Due to the small patch size, one can propose median filtration of the vanilla method to mitigate such attack influence. Consequently, we have conducted experiments on the median filtration of attacked images with different window sizes. From Table 5, we observe a decrease in FR, e.g., for EfficientNetB3 and 3×3 filter, we get a $1/3$ decrease for FR from the initial one; for some models like DenseNet161, the FR decreases to only

79%. However, as a hyperparameter, the filter size should be selected for each model and balance between efficient filtration and over-blurring.

Model	3x3	5x5	7x7	11x11	15x15
DN	95.32	97.03	94.97	79.66	88.25
ENB0	17.31	29.27	40.99	66.95	82.34
ENB3	9.13	16.54	24.07	41.70	59.33

Table 5: Fooling Rate (FR) after the median filtration results for three models: EfficientNetB0 (ENB0), EfficientNetB3 (ENB3) and DenseNet161 (DN). We see that median filtration helps to eliminate attacks, but the optimal window size is not the same for all models and should be tuned. Moreover, exceeding the optimal threshold results in over-blurring and a decrease in the performance of the model, not due to the attack but because of the bad quality of the images themselves.

To conclude, the median filter can make the attack harder to fool the victim model but does not protect from it entirely. More reliable way to protect models is to use attack detectors or/and robust normalizations inside the models; this requires additional training for each attack type which is impractical.

From/To	DN	ENB0	ENB3	IncV3	RN101	RN152	WRN101	DEIT	ViT
DenseNet161 (DN)	-	23.89	7.68	90.09	17.31	30.76	24.59	26.76	26.29
EfficientNetB0 (ENB0)	27.72	-	9.74	24.45	28.72	25.34	27.28	19.7	17.22
EfficientNetB3 (ENB3)	12.24	12.46	-	9.82	14.34	14.46	12.98	10.9	8.56
InceptionV3 (IncV3)	30.78	28.92	11.64	-	27.28	24.88	25.63	26.8	18.95
ResNet101 (RN101)	21.08	21.02	8.93	11.45	-	26.53	24.58	19.61	10.22
ResNet152 (RN152)	28.04	35.17	9.83	88.11	23.06	-	29.52	18.53	9.9
Wide ResNet101 (WRN101)	24.36	23.3	7.77	15.57	32.95	28.84	-	17.17	20.63
DEIT	17.82	17.24	7.31	9.65	25.57	18.88	20.33	-	9.8
ViT	23.87	23.13	8.5	14.28	28.29	21.06	20.96	13.64	-

Table 6: Transferability results for SV attack in terms of the Fooling Rate (FR). Rows refer to the model adversarial perturbation was computed on, while columns —to the victim one on which the attack was tested.

From/To	DN	ENB0	ENB3	IncV3	RN101	RN152	WRN101	DEIT	ViT
DenseNet161 (DN)	-	15.29	8.88	55.31	83.9	68.93	92.98	16.66	17.29
EfficientNetB0 (ENB0)	78.51	-	9.41	41.58	88.44	77.42	78.67	23.03	27.78
EfficientNetB3 (ENB3)	75.82	28.2	-	41.02	76.74	66.03	71.45	24.61	29.81
InceptionV3 (IncV3)	93.94	35.9	14.65	-	98.01	95.92	96.62	31.18	58.31
ResNet101 (RN101)	90.09	18.52	9.65	60.67	-	88.08	96.48	17.42	23.12
ResNet152 (RN152)	84.39	22.05	10.21	60.41	96.98	-	94.94	21.11	29.61
Wide ResNet101 (WRN101)	86.55	16.68	8.64	56.43	90.7	79.34	-	17.45	21.12
DEIT	75.36	40.64	10.64	51.32	75.97	71.12	80.2	-	31.2
ViT	77.27	22.12	10.19	63.72	98.28	97.19	94.85	32.79	-

Table 7: Transferability results for proposed TPower attack in terms of the Fooling Rate (FR). Rows refer to the model adversarial perturbation was computed on, while columns —to the victim one on which the attack was tested.

Transferability experiments. Following the above setup, in the transferability task, for each model we only consider the optimal perturbations in terms of FR obtained during the gridsearch. The rest of the evaluations are done on the test subset. In contrast to the direct task setting, when the adversarial perturbation is applied to the same model on which it was obtained, the attack should be adjusted to the input size of the victim model. In particular, we preprocess adversaries either centre-cropping or zero-padding them to fulfil the victim model input size restriction. Even though this affects the attack transferability performance, from Table 6 and Table 7, one can observe Tpower attack higher transferability across different models in the majority of cases.

Table 7 demonstrates that the most transferable attacks in terms of the fooling rate are the ones trained on transformers and EfficientNets. Moreover, EfficientNets are the most robust among examined models. In addition, for the rest surrogate models, attack is transferred almost equally well only among these architectures. This behaviour could be

explained by EfficientNet’s significant differences from all other models, as this architecture was not developed manually but using the AutoML MNAS framework. Nevertheless, attacks trained on EfficientNets have a sufficient transferability fooling rate of at least 24%, preserving the attacked picture’s good quality (see Figure 1) and outperforming the results for dense perturbations. It is worth mentioning that such attacks perform better in the transferability setting than in the direct one.

To sum up, the transferability of the proposed TPower approach makes it promising for a grey-box setting, where an attack is trained on one model and applied to an unknown one. However, it should be emphasized that a more detailed study and comparison of various DNN architectures should be done.

4 Related Work

In recent years, there have been numerous advancements in adversarial attacks. The concept of adversarial attacks in deep neural networks (DNNs) was first introduced in Szegedy et al. [2014]. To exploit this problem, Szegedy et al. used the L-BFGS algorithm. This finding significantly impacted the vision research community, which had previously believed that deep visual features closely approximated the perceptual differences between images using euclidean distances.

The Projected Gradient Descent (PGD) attack is regarded as one of the most potent attacks in the field Madry et al. [2017]. Their main contribution was to examine the adversarial robustness of deep models using robust optimization, which formalizes adversarial training of deep models as a min-max optimization problem.

Widely used adversarial machine learning techniques such as FGSM and DeepFool are designed to generate perturbations that target individual images to attack a specific network. In contrast, the universal adversarial perturbations Moosavi-Dezfooli et al. [2017] method introduces a unique approach by creating perturbations that have the potential ability to attack any image and any network.

Separately, we would like to highlight the class of attacks obtained using generative models Mopuri et al. [2018], Hayes and Danezis [2018], Poursaeed et al. [2018], Chen et al. [2023]. Such frameworks are well suited for creating attacks because GANs are able to learn the whole distribution of perturbations, and not just one perturbation as in non-generative approaches Mopuri et al. [2018].

To create a universal adversarial perturbation, an iterative approach is usually employed. Similar to the DeepFool algorithm Moosavi-Dezfooli et al. [2016b], the authors gradually shift a single data value towards its nearest hyperplane. In the case of UAP, this process is repeated for all input data points, pushing them towards their respective hyperplanes consecutively. The main problem with this approach is that it is computationally expensive.

Recent and relevant research includes Khruikov and Oseledets [2018], where the authors introduced a new algorithm for constructing universal perturbations. The algorithm is based on computing the (p, q) -singular values of Jacobian matrices of the network’s hidden layers. The authors utilized the well-known Power Method algorithm [Boyd, 1974] to compute the (p, q) -singular vectors. This idea has become popular not only in computer vision; the recent work adopts this algorithm for NLP problems as an example Tsymboi et al. [2023].

Since then, new gradient-based attacks have appeared, like flexible perturbation sets attacks Wong et al. [2019], Wong and Kolter [2020], as well as attacks with access only to the output scores of the classifier Guo et al. [2019a], Cheng et al. [2018], Wang et al. [2020], Guo et al. [2019b], Andriushchenko et al. [2020] and decision-based attacks with access only to predicted labels Chen et al. [2020].

Despite the rapid development of this area, universal attacks are still relatively rare. Many of them are based on generative models Sarkar et al. [2017], Mopuri et al. [2018], Poursaeed et al. [2018], Mao et al. [2020]. Recently, a trend in this area has appeared related to the representation of a universal attack as a semantic feature Zhang et al. [2020]. Following this work, a bridge between universal and non-universal settings was built Li et al. [2022].

5 Limitations and future work

One of the restrictions of the proposed approach is the fixed predefined attack cardinality, and due to the lack of convergence, heuristic reduction to this value should be made. One way to overcome this issue is to replace the truncation operator with adaptive threshold shrinkage obtained via the Alternating Direction Method of Multipliers (ADMM, Boyd et al. [2011]), which is planned to be done in future work.

Another weakness is that for sparse attacks to be efficient, we need to use higher magnitudes while keeping the percentage of damaged pixels low. As a result, adversarial perturbation could be considered as an outlier with

straightforward defence via weights clipping at each neural network layer. However, clipping ranges for this case must be well-estimated. We need to tune these parameters, e.g., estimate it based on statistics of layers outputs which is infeasible in the grey-box setting when the perturbation is transferred between models.

Finally, it would be interesting to investigate the sparse attack transferability in more realistic settings when both model and dataset are unknown, revealing task-independent adversarial perturbations.

6 Conclusion

This paper presents a new approach for sparse universal adversarial attack generation. Following Khruikov and Oseledets [2018], we assume that the perturbation of an intermediate layer propagates further through the network. The main outcome of the paper is that by using only an additional truncation operator, we can construct the perturbation that will alter at most 5% of input image pixels without a decrease in fooling rate compared to the dense algorithm version, but with a significant increase. Moreover, our attack is still efficient regarding the sample size used for perturbation training. In particular, utilizing 256 samples is enough to achieve at least a 50% fooling rate for the majority of models, with a maximum of 94%. We perform a comprehensive study of 10 architectures, revealing their vulnerability to sparse universal attacks. We also show that found attack vectors are highly transferable, revealing an extremely high vulnerability of ResNets. Furthermore, our attack can be well generalized across different networks without a decrease in the fooling rate.

References

- Alexey Dosovitskiy, Lucas Beyer, Alexander Kolesnikov, Dirk Weissenborn, Xiaohua Zhai, Thomas Unterthiner, Mostafa Dehghani, Matthias Minderer, Georg Heigold, Sylvain Gelly, Jakob Uszkoreit, and Neil Houlsby. An image is worth 16x16 words: Transformers for image recognition at scale, 2021a.
- Hugo Touvron, Thibaut Lavril, Gautier Izacard, Xavier Martinet, Marie-Anne Lachaux, Timothée Lacroix, Baptiste Rozière, Naman Goyal, Eric Hambro, Faisal Azhar, Aurelien Rodriguez, Armand Joulin, Edouard Grave, and Guillaume Lample. Llama: Open and efficient foundation language models, 2023.
- Hyung Won Chung, Le Hou, Shayne Longpre, Barret Zoph, Yi Tay, William Fedus, Yunxuan Li, Xuezhi Wang, Mostafa Dehghani, Siddhartha Brahma, Albert Webson, Shixiang Shane Gu, Zhuyun Dai, Mirac Suzgun, Xinyun Chen, Aakanksha Chowdhery, Alex Castro-Ros, Marie Pellat, Kevin Robinson, Dasha Valter, Sharan Narang, Gaurav Mishra, Adams Yu, Vincent Zhao, Yanping Huang, Andrew Dai, Hongkun Yu, Slav Petrov, Ed H. Chi, Jeff Dean, Jacob Devlin, Adam Roberts, Denny Zhou, Quoc V. Le, and Jason Wei. Scaling instruction-finetuned language models, 2022.
- Nicholas Roy, Ingmar Posner, Tim Barfoot, Philippe Beaudoin, Yoshua Bengio, Jeannette Bohg, Oliver Brock, Isabelle Depatie, Dieter Fox, Dan Koditschek, Tomas Lozano-Perez, Vikash Mansinghka, Christopher Pal, Blake Richards, Dorsa Sadigh, Stefan Schaal, Gaurav Sukhatme, Denis Thérien, Marc Toussaint, and Michiel Van de Panne. From machine learning to robotics: Challenges and opportunities for embodied intelligence, 2021.
- Alexei Baevski, Henry Zhou, Abdelrahman Mohamed, and Michael Auli. wav2vec 2.0: A framework for self-supervised learning of speech representations, 2020.
- Christian Szegedy, Wojciech Zaremba, Ilya Sutskever, Joan Bruna, Dumitru Erhan, Ian Goodfellow, and Rob Fergus. Intriguing properties of neural networks. In *International Conference on Learning Representations*, 2014. URL <http://arxiv.org/abs/1312.6199>.
- Ian J. Goodfellow, Jonathon Shlens, and Christian Szegedy. Explaining and harnessing adversarial examples, 2014. URL <https://arxiv.org/abs/1412.6572>.
- Seyed-Mohsen Moosavi-Dezfooli, Alhussein Fawzi, Omar Fawzi, and Pascal Frossard. Universal adversarial perturbations. In *Proceedings of the IEEE Conference on Computer Vision and Pattern Recognition (CVPR)*, July 2017.
- Valentin Khruikov and Ivan Oseledets. Art of singular vectors and universal adversarial perturbations. In *Proceedings of the IEEE Conference on Computer Vision and Pattern Recognition (CVPR)*, June 2018.
- David W Boyd. The power method for lp norms. *Linear Algebra and its Applications*, 9:95–101, 1974.
- Yang Song, Rui Shu, Nate Kushman, and Stefano Ermon. Constructing unrestricted adversarial examples with generative models. In S. Bengio, H. Wallach, H. Larochelle, K. Grauman, N. Cesa-Bianchi, and R. Garnett, editors, *Advances in Neural Information Processing Systems*, volume 31. Curran Associates, Inc., 2018. URL https://proceedings.neurips.cc/paper_files/paper/2018/file/8cea559c47e4fbd73b23e0223d04e79-Paper.pdf.

- Tom B Brown, Nicholas Carlini, Chiyuan Zhang, Catherine Olsson, Paul Christiano, and Ian Goodfellow. Unrestricted adversarial examples. *arXiv preprint arXiv:1809.08352*, 2018.
- Chengyin Hu and Weiwen Shi. Adversarial color film: Effective physical-world attack to dnns. *arXiv preprint arXiv:2209.02430*, 2022.
- Juncheng Li, Frank Schmidt, and Zico Kolter. Adversarial camera stickers: A physical camera-based attack on deep learning systems. In *International Conference on Machine Learning*, pages 3896–3904. PMLR, 2019.
- Mikhail Pautov, Grigorii Melnikov, Edgar Kaziakhmedov, Klim Kireev, and Aleksandr Petiushko. On adversarial patches: real-world attack on arcface-100 face recognition system. In *2019 International Multi-Conference on Engineering, Computer and Information Sciences (SIBIRCON)*, pages 0391–0396. IEEE, 2019.
- Edgar Kaziakhmedov, Klim Kireev, Grigorii Melnikov, Mikhail Pautov, and Aleksandr Petiushko. Real-world attack on mtcnn face detection system. In *2019 International Multi-Conference on Engineering, Computer and Information Sciences (SIBIRCON)*, pages 0422–0427. IEEE, 2019.
- Francesco Croce and Matthias Hein. Sparse and imperceivable adversarial attacks. In *Proceedings of the IEEE/CVF International Conference on Computer Vision*, pages 4724–4732, 2019.
- Apostolos Modas, Seyed-Mohsen Moosavi-Dezfooli, and Pascal Frossard. Sparsefool: a few pixels make a big difference, 2019.
- Zheng Yuan, Jie Zhang, Yunpei Jia, Chuanqi Tan, Tao Xue, and Shiguang Shan. Meta gradient adversarial attack. In *Proceedings of the IEEE/CVF International Conference on Computer Vision*, pages 7748–7757, 2021.
- Xiaoyi Dong, Dongdong Chen, Jianmin Bao, Chuan Qin, Lu Yuan, Weiming Zhang, Nenghai Yu, and Dong Chen. Greedyfool: Distortion-aware sparse adversarial attack. *Advances in Neural Information Processing Systems*, 33: 11226–11236, 2020.
- Nicolas Papernot, Patrick McDaniel, and Ian Goodfellow. Transferability in machine learning: from phenomena to black-box attacks using adversarial samples, 2016.
- Ziwen He, Wei Wang, Jing Dong, and Tieniu Tan. Transferable sparse adversarial attack. In *Proceedings of the IEEE/CVF Conference on Computer Vision and Pattern Recognition*, pages 14963–14972, 2022.
- Zeliang Zhang, Peihan Liu, Xiaosen Wang, and Chenliang Xu. Improving adversarial transferability with scheduled step size and dual example. *arXiv preprint arXiv:2301.12968*, 2023.
- Ali Shafahi, Mahyar Najibi, Zheng Xu, John Dickerson, Larry S Davis, and Tom Goldstein. Universal adversarial training. In *Proceedings of the AAAI Conference on Artificial Intelligence*, volume 34, pages 5636–5643, 2020.
- Francesco Croce, Maksym Andriushchenko, Naman D. Singh, Nicolas Flammarion, and Matthias Hein. Sparse-rrs: A versatile framework for query-efficient sparse black-box adversarial attacks. *Proceedings of the AAAI Conference on Artificial Intelligence*, 36(6):6437–6445, Jun. 2022. doi:10.1609/aaai.v36i6.20595. URL <https://ojs.aaai.org/index.php/AAAI/article/view/20595>.
- Jamie Hayes and George Danezis. Learning universal adversarial perturbations with generative models. In *2018 IEEE Security and Privacy Workshops (SPW)*, pages 43–49. IEEE, 2018.
- Konda Reddy Mopuri, Utkarsh Ojha, Utsav Garg, and R Venkatesh Babu. Nag: Network for adversary generation. In *Proceedings of the IEEE conference on computer vision and pattern recognition*, pages 742–751, 2018.
- Jia Deng, Wei Dong, Richard Socher, Li-Jia Li, Kai Li, and Li Fei-Fei. Imagenet: A large-scale hierarchical image database. In *2009 IEEE Conference on Computer Vision and Pattern Recognition*, pages 248–255, 2009a. doi:10.1109/CVPR.2009.5206848.
- Seyed-Mohsen Moosavi-Dezfooli, Alhussein Fawzi, and Pascal Frossard. Deepfool: A simple and accurate method to fool deep neural networks. In *2016 IEEE Conference on Computer Vision and Pattern Recognition (CVPR)*, pages 2574–2582, 2016a. doi:10.1109/CVPR.2016.282.
- Xiao-Tong Yuan and Tong Zhang. Truncated power method for sparse eigenvalue problems. *Journal of Machine Learning Research*, 14(4), 2013.
- Jia Deng, Wei Dong, Richard Socher, Li-Jia Li, Kai Li, and Li Fei-Fei. Imagenet: A large-scale hierarchical image database. In *2009 IEEE conference on computer vision and pattern recognition*, pages 248–255. Ieee, 2009b.
- Gao Huang, Zhuang Liu, Laurens Van Der Maaten, and Kilian Q Weinberger. Densely connected convolutional networks. In *Proceedings of the IEEE conference on computer vision and pattern recognition*, pages 4700–4708, 2017.
- Mingxing Tan and Quoc Le. Efficientnet: Rethinking model scaling for convolutional neural networks. In *International conference on machine learning*, pages 6105–6114. PMLR, 2019.

- Christian Szegedy, Wei Liu, Yangqing Jia, Pierre Sermanet, Scott Reed, Dragomir Anguelov, Dumitru Erhan, Vincent Vanhoucke, and Andrew Rabinovich. Going deeper with convolutions. In *Proceedings of the IEEE conference on computer vision and pattern recognition*, pages 1–9, 2015.
- Kaiming He, Xiangyu Zhang, Shaoqing Ren, and Jian Sun. Deep residual learning for image recognition. In *Proceedings of the IEEE conference on computer vision and pattern recognition*, pages 770–778, 2016.
- Karen Simonyan and Andrew Zisserman. Very deep convolutional networks for large-scale image recognition. In Yoshua Bengio and Yann LeCun, editors, *3rd International Conference on Learning Representations, ICLR 2015, San Diego, CA, USA, May 7-9, 2015, Conference Track Proceedings*, 2015. URL <http://arxiv.org/abs/1409.1556>.
- Sergey Zagoruyko and Nikos Komodakis. Wide residual networks. In Richard C. Wilson, Edwin R. Hancock, and William A. P. Smith, editors, *Proceedings of the British Machine Vision Conference 2016, BMVC 2016, York, UK, September 19-22, 2016*. BMVA Press, 2016. URL <http://www.bmva.org/bmvc/2016/papers/paper087/index.html>.
- Hugo Touvron, Matthieu Cord, Matthijs Douze, Francisco Massa, Alexandre Sablayrolles, and Hervé Jégou. Training data-efficient image transformers & distillation through attention. In *International conference on machine learning*, pages 10347–10357. PMLR, 2021.
- Alexey Dosovitskiy, Lucas Beyer, Alexander Kolesnikov, Dirk Weissenborn, Xiaohua Zhai, Thomas Unterthiner, Mostafa Dehghani, Matthias Minderer, Georg Heigold, Sylvain Gelly, Jakob Uszkoreit, and Neil Houlsby. An image is worth 16x16 words: Transformers for image recognition at scale. *ICLR*, 2021b.
- Il’ya Meerovich Sobol’. On the distribution of points in a cube and the approximate evaluation of integrals. *Zhurnal Vychislitel’noi Matematiki i Matematicheskoi Fiziki*, 7(4):784–802, 1967.
- Bichen Wu, Chenfeng Xu, Xiaoliang Dai, Alvin Wan, Peizhao Zhang, Zhicheng Yan, Masayoshi Tomizuka, Joseph Gonzalez, Kurt Keutzer, and Peter Vajda. Visual transformers: Token-based image representation and processing for computer vision, 2020.
- Aleksander Madry, Aleksandar Makelov, Ludwig Schmidt, Dimitris Tsipras, and Adrian Vladu. Towards deep learning models resistant to adversarial attacks. *arXiv preprint arXiv:1706.06083*, 2017.
- Omid Poursaeed, Isay Katsman, Bicheng Gao, and Serge Belongie. Generative adversarial perturbations. In *Proceedings of the IEEE conference on computer vision and pattern recognition*, pages 4422–4431, 2018.
- Zhaoyu Chen, Bo Li, Shuang Wu, Kaixun Jiang, Shouhong Ding, and Wenqiang Zhang. Content-based unrestricted adversarial attack. *arXiv preprint arXiv:2305.10665*, 2023.
- Seyed-Mohsen Moosavi-Dezfooli, Alhussein Fawzi, and Pascal Frossard. Deepfool: a simple and accurate method to fool deep neural networks. In *Proceedings of the IEEE conference on computer vision and pattern recognition*, pages 2574–2582, 2016b.
- Olga Tsymboi, Danil Malaev, Andrei Petrovskii, and Ivan Oseledets. Layerwise universal adversarial attack on nlp models. In *Findings of the Association for Computational Linguistics: ACL 2023*, pages 129–143, 2023.
- Eric Wong, Frank Schmidt, and Zico Kolter. Wasserstein adversarial examples via projected sinkhorn iterations. In *International Conference on Machine Learning*, pages 6808–6817. PMLR, 2019.
- Eric Wong and J Zico Kolter. Learning perturbation sets for robust machine learning. *arXiv preprint arXiv:2007.08450*, 2020.
- Yiwen Guo, Ziang Yan, and Changshui Zhang. Subspace attack: Exploiting promising subspaces for query-efficient black-box attacks. *Advances in Neural Information Processing Systems*, 32, 2019a.
- Minhao Cheng, Thong Le, Pin-Yu Chen, Jinfeng Yi, Huan Zhang, and Cho-Jui Hsieh. Query-efficient hard-label black-box attack: An optimization-based approach. *arXiv preprint arXiv:1807.04457*, 2018.
- Lu Wang, Huan Zhang, Jinfeng Yi, Cho-Jui Hsieh, and Yuan Jiang. Spanning attack: Reinforce black-box attacks with unlabeled data. *Machine Learning*, 109:2349–2368, 2020.
- Chuan Guo, Jacob Gardner, Yurong You, Andrew Gordon Wilson, and Kilian Weinberger. Simple black-box adversarial attacks. In *International Conference on Machine Learning*, pages 2484–2493. PMLR, 2019b.
- Maksym Andriushchenko, Francesco Croce, Nicolas Flammarion, and Matthias Hein. Square attack: a query-efficient black-box adversarial attack via random search. In *European conference on computer vision*, pages 484–501. Springer, 2020.
- Jianbo Chen, Michael I Jordan, and Martin J Wainwright. Hopskipjumpattack: A query-efficient decision-based attack. In *2020 IEEE Symposium on Security and Privacy (SP)*, pages 1277–1294. IEEE, 2020.

- Sayantana Sarkar, Ankan Bansal, Upal Mahbub, and Rama Chellappa. Upset and angri: Breaking high performance image classifiers. *arXiv preprint arXiv:1707.01159*, 2017.
- Xiaofeng Mao, Yuefeng Chen, Yuhong Li, Yuan He, and Hui Xue. Gap++: Learning to generate target-conditioned adversarial examples. *arXiv preprint arXiv:2006.05097*, 2020.
- Chaoning Zhang, Philipp Benz, Tooba Imtiaz, and In So Kweon. Understanding adversarial examples from the mutual influence of images and perturbations. In *Proceedings of the IEEE/CVF Conference on Computer Vision and Pattern Recognition*, pages 14521–14530, 2020.
- Maosen Li, Yanhua Yang, Kun Wei, Xu Yang, and Heng Huang. Learning universal adversarial perturbation by adversarial example. In *Proceedings of the AAAI Conference on Artificial Intelligence*, volume 36, pages 1350–1358, 2022.
- Stephen Boyd, Neal Parikh, Eric Chu, Borja Peleato, Jonathan Eckstein, et al. Distributed optimization and statistical learning via the alternating direction method of multipliers. *Foundations and Trends® in Machine learning*, 3(1): 1–122, 2011.
- Kenneth T Co, Luis Muñoz-González, Leslie Kanthan, Ben Glocker, and Emil C Lupu. Universal adversarial robustness of texture and shape-biased models. In *2021 IEEE International Conference on Image Processing (ICIP)*, pages 799–803. IEEE, 2021.

A Implementaion details

Image preprocessing. The preprocessing stage is a crucial step in computer vision tasks that involves cleaning, standardizing, and enhancing the input data to improve model performance. In the context of these experiments, the preprocessing pipeline for the ImageNet ILSVRC2012 dataset will be discussed.

At first, we divided the ImageNet dataset between a training subset with 256 images, a validation subset of 5000 images and the rest for the test subset. The second step in the preprocessing pipeline involves resizing the input images to a fixed resolution. This is necessary to ensure that all images have the same dimensions and to reduce the computational overhead of training the models. The images will be resized to a resolution of crop sizes corresponding to the used models. After that, our actions for the subsets are different. We compute the attack tensor on the normalized train subset. We apply an attack on validation and test subsets.

Overall, the preprocessing pipeline for the ImageNet ILSVRC2012 dataset for our experiments consists of the train-validation-test split, resizing/cropping, attack applying, clipping to $[0, 1]$ (for validation and test subset) and normalization.

Layer selection. We gradually went through all semantic blocks to study the performance dependence on the layer to be attacked:

- DenseNet161: dense layers and transition blocks,
- EffecientNetB0 and EffecientNetB3: bottleneck MBConv blocks,
- InceptionV3: max poolings and mixed blocks,
- ResNet101, ResNet152 and WideResNet101: residual blocks,
- Vit and DEIT: encoder layers.

B Experiments

Grid search results for SV attack. Optimal hyperparameters with corresponding fooling and attack success rates are presented in Table 8. Figure 8 present examples of dense adversarial perturbations. For optimal layers regarding the fooling rate, the dependence on q is ambiguous, while on average, the hypothesis that the greater q is, the better attack performance is Khrulkov and Oseledets [2018] not approved.

Model	q	Attacked Layer	Test ASR	Test FR
DenseNet161	3	features.denseblock2.denselayer10	26.49	34.25
EffecientNetB0	5	features.2.1.block	26.58	34.44
EffecientNetB3	2	features.1.0.block	8.3	13.49
InceptionV3	2	Mixed_5b	19.64	27.88
ResNet101	5	layer1.0	43.54	50.05
ResNet152	5	layer1.0	28.58	35.93
WideResNet101	1	layer3.1	29.24	36.35
DEIT base	3	vit.encoder.layer.1	23.23	31.1
ViT base	5	vit.encoder.layer.0	18.75	26.01

Table 8: Metrics and hyperparameters for the best-performed SV attacks for each model. The attack magnitude was fixed at $\alpha = \frac{10}{255}$.

Dependence on patch size. In general, from Table 3, one can see that pixel-wise attack mode is more efficient regarding the fooling rate. This might be related to the fact that uniform square greed is not an optimal sparsity pattern. However, for most models, the decrease in performance is not dramatic, except for the transformers one.

SGD with layer maximization. We also conducted additional experiments and decided to compare with SGD layer maximization attack Co et al. [2021], essentially an unlinearized version of our algorithm. The results are presented in 9, and attack samples are presented in 7. As we can observe, layer maximization significantly boosts classic stochastic gradient descent, but the attack still does not reach the performance of our attack or SV attack.

Model	Ours	SV	SGD	LMax
DenseNet161	89.11	34.25	15.53	23
EffecientNetB0	37.09	34.44	16.35	19.12
EffecientNetB3	15.22	13.49	8.22	11.21
InceptionV3	85.04	27.88	13.11	24.64
ResNet101	94.57	50.05	17.17	46.95
ResNet152	94.84	35.93	15.05	22.49
WideResNet101	94.36	36.35	15.02	28.42
DEIT base	43.37	31.1	19.16	23.55
ViT base	52.5	26.01	17.09	28.09

Table 9: Metrics for each model with SGD layer maximization attack. The attack magnitude for dense attacks was fixed at $\alpha = \frac{10}{255}$.

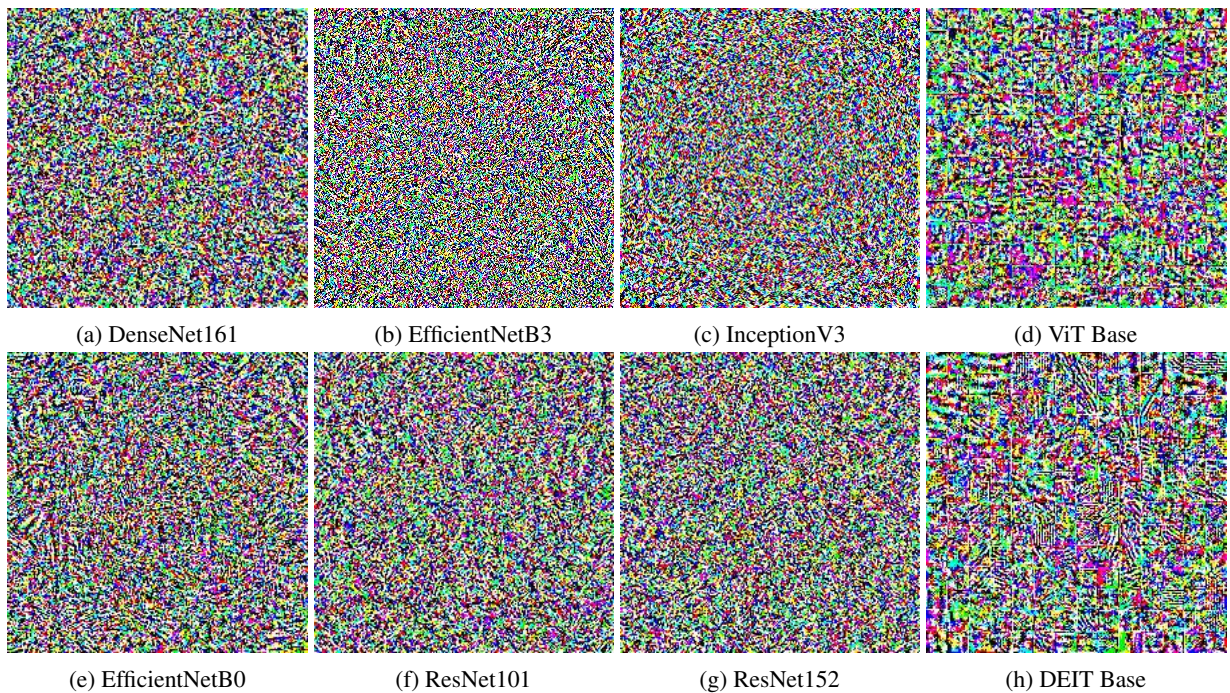


Figure 6: UAPs obtained using SGD attack algorithm Shafahi et al. [2020].

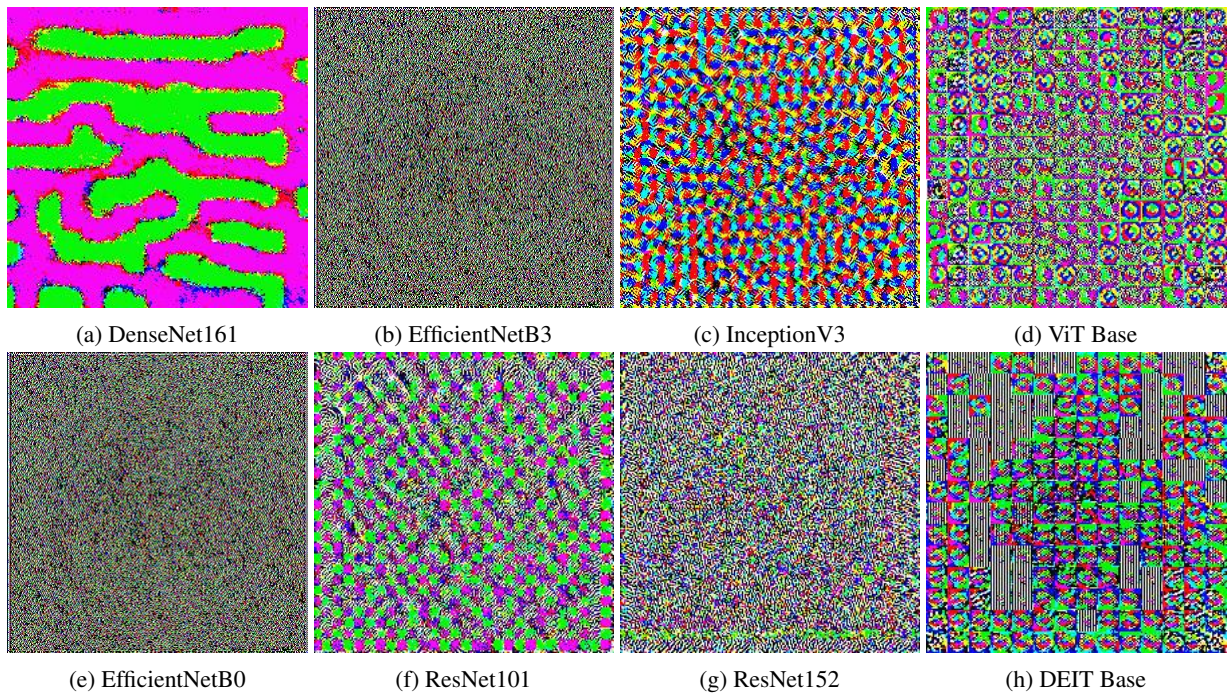


Figure 7: UAPs obtained using SGD with layer maximization attack algorithm Co et al. [2021]. Selected layers are the same as optimal in TPower attack.

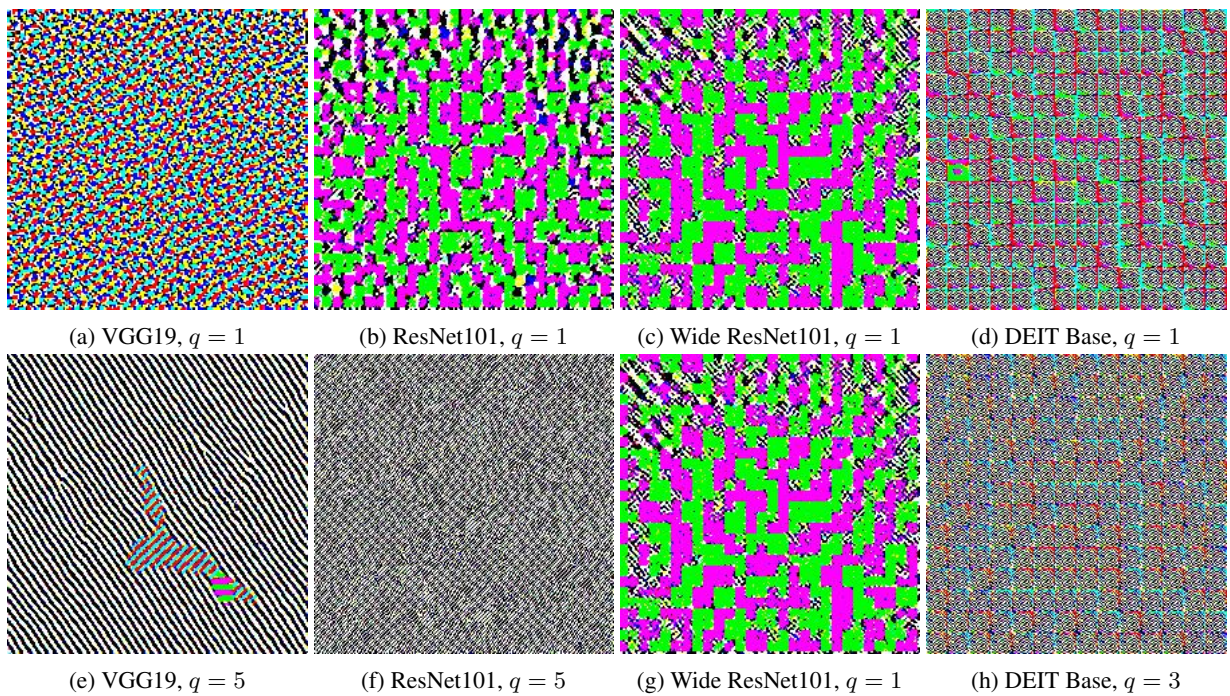


Figure 8: UAPs using SV attack algorithm Khruklov and Oseledets [2018]. The first row refers to the fixed parameter value $q = 1$, while the second depicts best-performed perturbations.

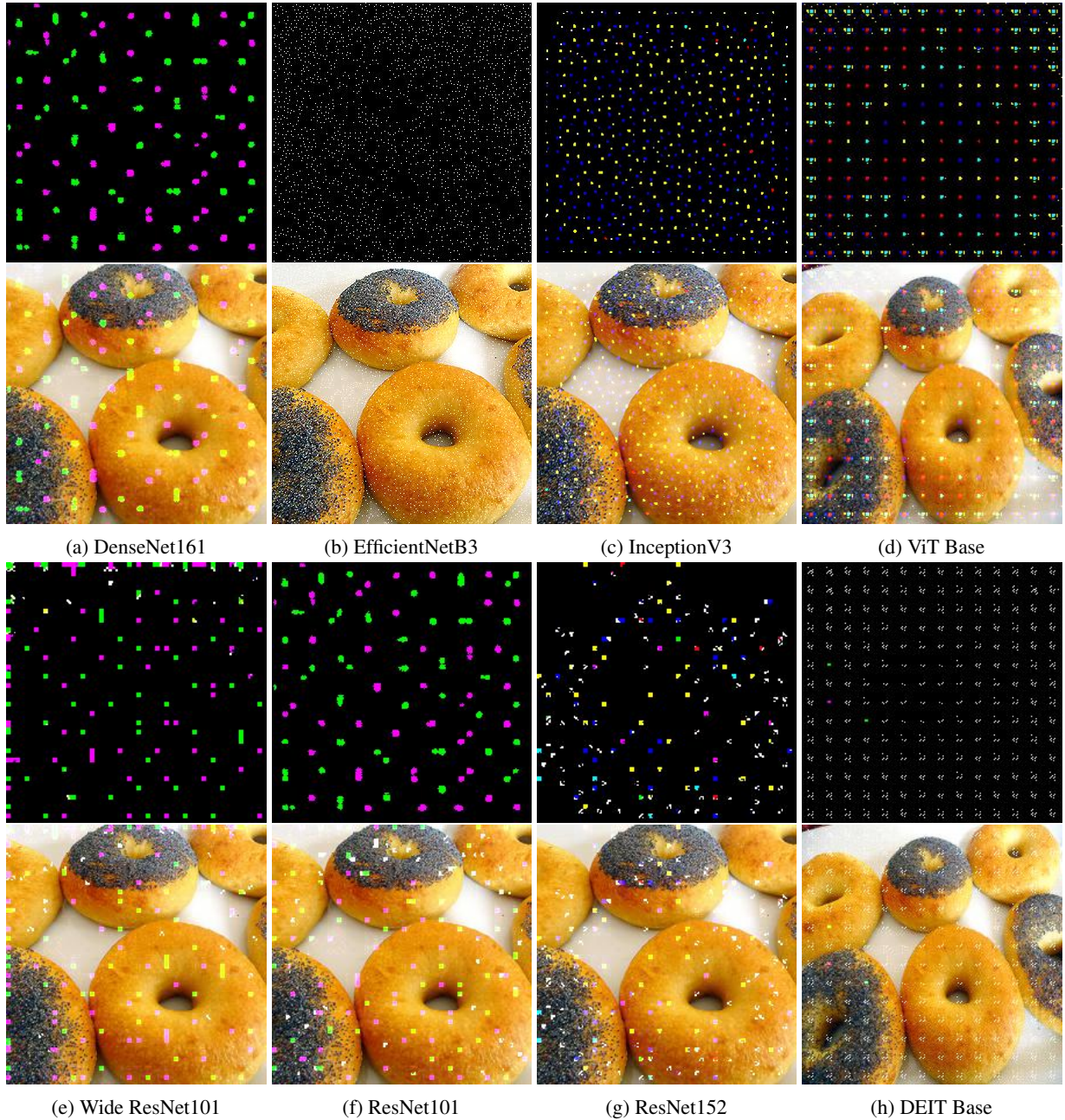


Figure 9: UAPs and corresponding attacked images obtained using our TPower approach. Perturbations were computed using the best-performed layers on gridsearch.